Performance And Emissions Modeling Of Natural Gas Dual Fuelling Of Large Diesel Engines

Peter L. Mtui

ABSTRACT: This paper presents numerical investigations the combustion characteristics and maximum possible natural gas substitution on a large stationary diesel engine dual fuelled with natural gas operation at 600 RPM. The performance effect in the dual fuel diesel engines is investigated using the coupled 1D/3D computer simulation of GT-POWER and KIVA-3 computer codes for combustion optimization and emissions reduction. Numerical modeling was performed by varying engine load conditions from 100% to 77%, while with increasing the quantity of natural gas substitution from up to 80%. The main target of this contribution is to examine the combustion characteristic of a heavy duty 18 cylinder, 6 MW electricity generator diesel engine operating in dual fuel mode at various engine loads. Results indicate that up to 80% natural gas substitution is possible over wide range of engine load conditions at higher engine loads. However, for 77% engine load conditions depict noticeable engine performance deterioration above 60% natural gas deterioration, of particular, is higher BSFC and excessive CO emissions. Compared with straight diesel, the in-cylinder NOx formation was significantly reduced by as the quantity of natural gas substitution was increased. For example, NOx was reduced by 50% while engine at 80% engine load fuelled with 60% natural gas substitution. This is consistent with the reduced peak flame temperature observed in the combustion chamber, and that was confined with the fuel spray zone.

Keywords: GT-Power, KIVA, engine performance, diesel, natural gas, dual fuel, simulation

1. INTRODUCTION

It is well documented that the petroleum fuel reserves in the world are diminishing at an alarming rate and that an alternative fuel need to be sought for. Natural gas (NG) has been recognized to be one among the promising alternative to diesel fuel for stationary and transport engine vehicles because it emits lower levels of pollution compare to other fossil fuels. The use of natural as alternative fuel has been growing in recent years due to the considerable economic and environmental advantages and therefore, become more conventional fuel in internal combustion engines [12]. Natural gas can easily adaptable to spark-ignition (SI) engines, but not to a conventional compression ignition (CI) engine because NG will not auto-ignite in a conventional diesel engine due to its higher cetane number. However, diesel engines can be converted to run on gas either by conversion to spark-ignition (SI conversion), or by dual fuelling so that pilot diesel initiates combustion. Therefore, in order to realize the benefits of use of NG as fuel in internal combustion engines (ICE), it is necessary to understand the in-cylinder combustion under different engine operating conditions, as well understanding useful properties and characteristics of natural gas which are shown in Table 1.

- *Peter L. Mtui*
- *College of Engineering and Technology, University of Dar es Salaam, P. O. Box 35131, Dar es Salaam, Tanzania*
- *Email: plmtui@yahoo.com*

Table 1: Properties of natural gas [4]

Parameter	Value
Density (kg/m^3)	0.72
Flammability limit (volume % in air)	4.3 – 15
Flammability limit (equivalence ratio)	0.4 – 1.6
Autoignition temperature (^{0} C)	723
Octane rating	130
Cetane rating	42
Minimum ignition energy (MJ)	0.28
Flame velocity (m/s)	0.28
Adiabatic flame temperature (K)	2214
Quenching distance (mm)	2.1
Soichiometric fuel/air mass ratio	0.069
Stoichiometric volume fraction (%)	9.48
Lower heating value (MJ/kg)	45.8

The higher ignition temperature of NG compared with gasoline or diesel makes it less hazardous. Natural gas octane rating (120) is higher than that of gasoline (87) which allows higher compression ratio CR for spark-ignited engines up to 16:1 without “knock”, consequently increased thermal efficiency and fuel consumption and without knock or detonation. Diesel engines can be converted to run on NG either by conversion to spark-ignition (SI conversion), or by dual fuelling, pilot diesel provide ignition assistance because NG will not auto-ignite in a conventional diesel engine. In dual pilot diesel engine, Ouellette et al [13] developed high pressure direct injection (HPDI) of natural gas in diesel engines; results show about 40% NOx reduction compared with diesel operation. Today, natural gas engines can be categorized as the traditional premixed charge spark-ignited engine (fumigation), port injection, the high pressure dual fuel (pilot) direct injection. Recent research work has shown the direct injection is the most promising yielding almost comparable power and higher efficiency over diesel fuelled CI engine [10]. Chiu [3]

reported that although there are some drawbacks with respect to performance with spark-ignited engines, majority of natural gas engines today are premixed charge spark-ignited engines. Spark ignited engines have significant advantages over diesel engines in terms of particulate emissions. However, premixed spark-ignited engines suffer high pumping throttling losses resulting in 15 to 30% reduction in volumetric efficiency compared to compression-ignited engines [2]. In addition, natural gas fuelled SI engines suffer power output losses up to 30% compared to an equivalent size diesel engines due to knock limitations [10]. Shenghua et al [17] carried out experimental study on the combustion characteristics of turbocharged on natural gas pilot-ignited diesel engine. It is reported that an increase in pilot diesel quantity extends the lean limit and decrease the HC and CO emissions, however, NOx emissions was found to increase as the pilot diesel is increased.

2 MATERIALS AND METHOD

A heavy duty 18-cylinder, 6MW diesel engine has been modeled dual-fuelled with natural gas and pilot diesel to assist ignition. The engine specifications are shown in Table 2. Modeling procedure starts by entering the engine data to the GT-Power code for all engine components data such as manifolds, etc. At the same time, all parameters related to in-cylinder combustion including piston geometry and dual fuelling system was input to the KIVA-3 code. The two codes were activated and run concurrently to the final results.

Table 2: Engine Data

Parameter	Value
Rated power (MW)	6
Engine speed [rpm]	600
Number of cylinders	18
Cylinder bore, b, [mm]	320
Piston stroke, s, [mm]	420
Intake valve	
Open (deg BTDC)	75
Close (deg ABDC)	35
Exhaust valve	
Open (deg BBDC)	45
Close (deg ABTD)	35
Compression ratio	14

2.1 Performance of Diesel Engine

Engine geometric parameters are important on engine performance such as brake thermal efficiency, mechanical efficiency and volumetric efficiency as well as the mean effective pressure, specific power output and specific fuel consumption [9]. Volumetric efficiency is very important for four-stroke engines which have distinct suction stroke and therefore indicates the breathing ability of the engine. Ganesan [5] reported that the normal range of volumetric efficiency at full throttle for SI engines ranges 80% to 85% and for CI engines 85% to 90%. Discussed below are major engine performance parameters.

Mean effective pressure: Mean effective pressure (MEP) is shown in equation (1) where P is engine power and n_R is the number of crank revolutions for each power stroke per cylinder ($n_R = 1$ for two-stroke and $n_R = 2$ for four-stroke cycles).

$$MEP = \frac{P\, n_R}{V_d\, N} \tag{1}$$

Specific fuel consumption: For fuel mass flow rate, m_f, the specific fuel consumption sfc is given as:

$$sfc = \frac{m_f}{P} \tag{2}$$

Thermal efficiency: For given engine power P and fuel heating value Q_{HV}, the engine thermal efficiency η_{th} is:

$$\eta_{th} = \frac{P}{m_f\, Q_{HV}} \tag{3}$$

Engine power: The engine power is given in equation (4) where η_v is volumetric efficiency, V_D is engine displacement, ρ_a is air density and (F/A) is the fuel air ratio.

$$P = \frac{\eta_{th}\, \eta_v\, V_D\, Q_{HV}\, \rho_a\, (F/A)}{2} \tag{4}$$

The above performance parameters illustrate the direct importance to engine performance on high fuel conversion efficiency, high volumetric efficiency, increasing displacement engine size and increasing the inlet air density by charge cooling.

2.2 The 1D Engine Modeling

Presently in an engine system simulations have been reported to be performed by one-dimensional software in order to assess the effects of different geometrical and part changes on the system as a whole. These simulations are usually fast and multiple parameters can be monitored and analyzed (GT-Power, 2005).The GT-Power software simulates different engine components including pipes and flow splits that are used to build up the engine geometry. More specialized parts such as cylinders, turbochargers use in-built models to calculate the performance parameters such as cylinder pressure, heat release, and thermal efficiency. At its core, the GT-Power solver is based on the 1D solution of the fully unsteady, nonlinear Navier-Stokes equations. Beyond this software core is the thermodynamic and phenomenological model solvers to capture the effects such as combustion, heat transfer and droplet evaporation.

2.3 The 3D in-Cylinder Combustion

The 3-dimensional modeling of flow and combustion processes in the engine cylinder was performed using KIVA-3. The KIVA-3 computer code was coupled with the 1-dimensional (GT-Power code) to provide accurate boundary conditions of the intake and exhaust valves transient events. That is, the pressure oscillation behavior of all gas engine plenum and piping system outside the 3D domain of the engine cylinder is considered by the 1D model and therefore modeled by GT-Power. The 1D-3D analysis results in deeper understanding of complex flow phenomena in shorter time and engine performance can be evaluated immediately; for example, volumetric efficiency, fuel economy and engine power. Among the various engine simulation codes, the KIVA-3 code is the most widely used in engine research community. KIVA-3 is used as a base CFD code on which various physical and chemistry models are developed. KIVA-3 is a software package that numerically solves the transport equations of turbulent chemically reactive mixture of ideal gas with a single evaporating spray [1]. Turbulence is modeled by a modified renormalized group (RNG) of $k-\varepsilon$ which was first developed by Han and Reitz [7] and [8] to model the in-cylinder turbulence. This model takes into account the effects of spray compressibility and interaction with turbulence. The RNG model has shown to predict large-scale flame structures, therefore better prediction of the in-cylinder temperature flow field and NOx formation compared to the standard $k-\varepsilon$ turbulent model. The following section will describe diesel droplet breakup and collision followed with the chemical kinetics used to simulate diesel spray ignition, combustion and emissions formation.

2.3.1 Droplet Breakup

For droplet breakup, there are three main droplet breakup mechanisms that have been reported in literature. The Lagrangian spray models of Reitz and Diwakar [16] have been most widely used for more than two decades and is implemented in the KIVA-3 for modeling diesel droplet breakup. O'Rourke and Amsden [11] developed a *Taylor Analogy Breakup (TAB)* model for droplet beak-up. This is based on an analogy between an oscillating and distorting drop that penetrates through surrounding gas with a relative velocity u_{rel} and a forced oscillating spring-mass system. The aerodynamic drag acts as the external force to the drop, the liquid viscosity as the damping force and the surface tension as the restoring force. Based on this analogy, the equation for the acceleration of the droplet distortion parameter y is:

$$\ddot{y}+C_d\frac{\mu_l}{\rho_l r^2}\dot{y}+C_k\frac{\sigma}{\rho_l r^3}y=\frac{C_F}{C_b}\frac{\rho_g u_{rel}^2}{\rho_l r^2} \qquad (5)$$

where y is the normalized displacement of the droplet's from its equilibrium position C_d , C_k, C_b and C_F are model constants. r is the droplet radius. ρ_g and ρ_l are the gas and liquid densities, and σ is the surface tension. For each breakup event, the radius of the product drops is chosen randomly from χ-squared distribution. The number of the product drops can then be determined using mass conservation. The size of the product droplets is estimated using an energy balance.

2.3.2 Droplet Collision

The present study follows the drop collision model of O'Rourke and Bracco [12] in which droplet collision and coalescence are modeled using a statistical approach. The outcome of collision in practice leads into the formation of many new droplet parcels, causing rapid increase of droplets which requires excessive computer storage requirement. This is overcome by the use of statistical approach, that is, collision only occurs between a pair of droplet parcels provided they are in the same computational cell in which the droplets are also assumed to be uniformly distributed.

2.3.3 Drop Vaporization

The vaporization of liquid fuel influences ignition, combustion, and formation of pollutants. The vaporization process involves heat and mass transfer that will affect temperature, velocity, and vapor concentration in the gas phase. The standard modeling approach is to use a single component vaporization model, diesel. The rate of the drop temperature change is described as:

$$\frac{4\pi r^3}{3}\rho_d c_l\frac{dT_d}{dt}=4\pi r^2 Q_d+\rho_d 4\pi r^2\frac{dr}{dt}L_d \qquad (6)$$

where c_l is the specific heat of the liquid droplet, r is the radius of the, L is the latent heat of vaporization and Q_d is the rate of heat transfer by conduction to drop surface per unit area using the Ranz-Marshall correlation [18]

2.3.4 Heat Transfer

Han and Ritz (1997) developed a wall heat transfer model from the assumption of one-dimensional energy conservation equation. The gas-wall convective heat transfer model is dependent on the temperature wall function as well as variation of gas density and turbulent Prandtl number in the boundary layer. This model is reported to show improved accuracy with relatively coarse grids. The expression for heat flux q_w is given as:

$$q_w=\frac{\rho c_p u' T\left(\frac{T}{T_w}\right)}{2.1\ln\left(y'\right)+2.513} \qquad (7)$$

where $y'=\frac{u' y}{\nu}$ and $u'=C_\mu^{1/4}\,k^{1/2}$

and ρ is gas density, c_p is specific heat at pressure, μ is molecular viscosity, k is turbulent kinetic energy, T and

T_w is the gas and wall temperature, respectively. $C\mu$ is the RNK $k-\varepsilon$ turbulent model constant (0.0845).

2.3.5 NOx formation in Engine Emissions

The most important NOx formation mechanism is the Zeldovich mechanism, also called the thermal mechanism since this is responsible for the strong temperature dependence of NOx emissions. The mechanism was proposed by Zeldovich in 1946 (equations 8 to 10). As long as the maximum combustion temperature is fairly high (above ~2000 K), the Zeldovich mechanism is dominating the NO production. Internal combustion engines can typically not avoid high temperature regions in its entire operational range and therefore the Zeldovich mechanism is often considered to be dominating.

$$O + N_2 \Leftrightarrow NO + N \quad (8)$$

$$N + O_2 \Leftrightarrow NO + O \quad (9)$$

$$N + OH \Leftrightarrow NO + H \quad (10)$$

From the above three Zeldovich equations, Heywood [9] expressed the rate of NO formation in a single equation:

$$\frac{d[NO]}{dt} = 2k_{1f}[O][N_2]\frac{1-[NO]^2/\left(K[O_2][N_2]\right)}{1+k_{1b}[NO]/\left(k_{2f}[O_2]+k_{3f}[OH]\right)} \quad (11)$$

$$K = \frac{k_{1f}}{k_{1b}}\frac{k_{2f}}{k_{2b}}$$

where k is the reaction rate constant; the subscripts f and b are the forward and reverse reaction directions, respectively. The square brackets represent species molar concentrations.

2.3.6 Modeling Fluid Flow

The transport phenomena during engine combustion is turbulent and complex because of heat and mass transfer and chemical reaction mechanism during the in-cylinder cycle process. This process is governed by the conservation equations of mass, momentum, energy and species. Turbulence is modeled using the $k-\varepsilon$ equation.

Conservation of Mass

$$\frac{\partial\rho}{\partial t}+\frac{\partial}{\partial x_j}(\rho u_j)=S_c \quad (12)$$

where ρ and u are the gas density and velocity, and is mass source term. S_c is the mass source term.

Conservation of Momentum

$$\frac{\partial}{\partial t}(\rho u_i)+\frac{\partial}{\partial x_j}(\rho u_i u_j)=-\frac{\partial p}{\partial x_i}+\frac{\partial}{\partial x_j}\left(\mu\left(\frac{\partial u_i}{\partial x_j}+\frac{\partial u_i}{\partial x_i}\right)\right)+F_i \quad (13)$$

where p is the operating pressure, μ viscosity and F_i is sum of the forces.

Conservation of Energy

$$\frac{\partial}{\partial t}(\rho h)+\frac{\partial}{\partial x_j}(\rho u_i h)=\frac{\partial}{\partial x_j}\left(\frac{\mu}{\sigma_h}\frac{\partial h}{\partial x_j}\right)-q_r+S_h \quad (14)$$

where h is specific enthalpy, q_r and S_h are thermal radiation and energy source terms, respectively.

Conservation of Species

$$\frac{\partial}{\partial t}(\rho Y)+\frac{\partial}{\partial x_j}(\rho u_i Y)=\frac{\partial}{\partial x_j}\left(\frac{\mu}{\sigma_h}\frac{\partial Y}{\partial x_j}\right)+S_c \quad (15)$$

where Y is species concentration

Generation of Turbulence Kinetic Energy

$$\frac{\partial}{\partial t}(\rho k)+\frac{\partial}{\partial x_j}(\rho u_j k)=\frac{\partial}{\partial x_j}\left(\frac{\mu}{\sigma_k}\frac{\partial k}{\partial x_j}\right)+G_k+G_b+\rho\varepsilon \quad (16)$$

where k is turbulent kinetic energy and ε is dissipation rate of turbulent kinetic energy.

Dissipation of Turbulence Kinetic Energy

$$\frac{\partial}{\partial t}(\rho\varepsilon)+\frac{\partial}{\partial x_j}(\rho u_j\varepsilon)=\frac{\partial}{\partial x_j}\left(\frac{\mu}{\sigma_\varepsilon}\frac{\partial k}{\partial x_j}\right)+\frac{\varepsilon}{k}\left(C_1G_k-C_2\rho\varepsilon\right) \quad (17)$$

where G_k is the production of turbulence kinetic energy due to mean velocity gradients and G_b is the production of turbulence kinetic energy due to buoyancy. The above equations are discretized and solved iteratively by KIVA-3 code to obtain the flow field in the cylinder computational domain. The computational mesh was created from the piston geometry by considering on 60^0 sector mesh. Modeling just one one-sixth of the cylinder results into large reduction computer memory and CPU time requirement. The discretized computational domain contained approximately 120,000 cells.

3. RESULTS AND DISCUSSIONS

The engine combustion and performance parameters are discussed for the for GT-POWER simulation coupled with KIVA-3 cylinder. During simulation, the engine speed was kept constant at 600 rpm while the load was varied from 100% to 77%. Under these load and speed conditions, the quantity of natural gas (NG) substitution was varied from 0% to 80% in order to evaluate the effect of the quantity of NG substation with engine performance. The engine test loads were varied from 100%, 85%, 77% and 50% and are designated as L100, L85, L77 and L50, respectively. The in-cylinder temperature distribution and NOx formation as well as the unburned NG are presented. The engine power shown in Figure 1 for natural gas substitution up to about 60% nearly matches the engine power that of straight diesel. This is attributed mainly due to the fact that that better air-fuel mixture preparation for the case of natural gas fumigated engines and the low engine speed that provides enough time for combustion. Figure 2 depicts the trend of brake specific fuel consumption (bsfc). The results indicate worsening of bsfc as NG substitution is increased, particularly at above 50% natural gas substitution beyond which engine misfiring may occur. Shown in Figure 3 is the efficiency of trapped fresh charge which depicts decreasing efficiency as the NG substitution is increased. As a result, the volumetric efficiency decreases as indicated in Figure 4. This decreasing trend is mainly attributed to the induced natural gas occupying volume which otherwise would have been occupied by air. This trend is consistent with decreasing volumetric efficiency as NG substitution is increased. The contour plot depicted in Figure 5 represents the in-cylinder temperature distribution at engine load 85%, straight diesel 100% and with 0% natural gas substitution. Results indicate maximum temperature 2814 K which is localized near the diesel injector. The localized high temperature indicates stoichiometric combustion takes place in the vicinity of fuel injector location. Figure 6 shows temperature distribution at the same engine condition but with 60% natural gas substitution. Results indicate maximum temperature is about 2761 K which is lower than for the counterpart 100% diesel. This temperature trend is consistent with lower adiabatic flame temperature for natural gas. Another observation in Figure 6 is that, with NG substitution, the flame zone extends further to the radial direction of the piston bore compared to the counterpart 100% diesel. NOx formation is depicted in Figures 7 and 8 for engine load 85%, straight diesel 100% with 0% natural gas substitution. Results indicate that NOx concentration (mass fraction) for 100% diesel is 0.08762 while for and 60% natural gas substitution it is reduced to 0.0657. Both results illustrate that NOx formation occurs near zones of high temperature in the vicinity of the diesel injector. The contour plots in Figures 9 and 10 show the distribution of unburned natural gas (methane) in the engine piston bowl for engine load 85%, diesel 40% with 60% natural gas substitution. Results indicate that the unburned NG concentration (mass fraction) for 40% diesel is 0.0000133 and for 60% natural gas substitution is 0.0000681. The trends of unburned natural are consistent NG substitution, that is, larger quantities of NG substation leads into increased unburned NG due to unstable combustion which does not complete the fuel consumption. Note that Figure 9 depicts the unburned NG in the vicinity of cylinder head, however, the quantity is negligibly small, about 13.3 ppm.

4. CONCLUSION

Large engine simulation of pilot diesel and natural gas fuelled engine has been performed successfully using GT-Power and KIVA-3 engine codes. From these results, it is concluded that NG can be used as an alternative fuel into large stationary diesel engines successfully up to 60% NG substitution. The studied parameters show that the engine power remains nearly constant for natural gas substitution up to 40% beyond which the engine power decreases with high quantities of NG substitution. Further, if NG is increased beyond 50% the brake specific fuel consumption (bsfc) start to deteriorate. Large quantities of NG, for example 80% substitution results into unburned NG consequently poor bsfc as well as excessive emissions of unbured hydrocarbons and CO. The in-cylinder temperature distribution indicates marked higher temperature for straight diesel engine compared with the case of partial natural gas substitution. For example, 60% natural gas substitution at 85% engine load leads into about 53 K temperature reduction, consequently the peak NOx formation was reduce by about 24%.

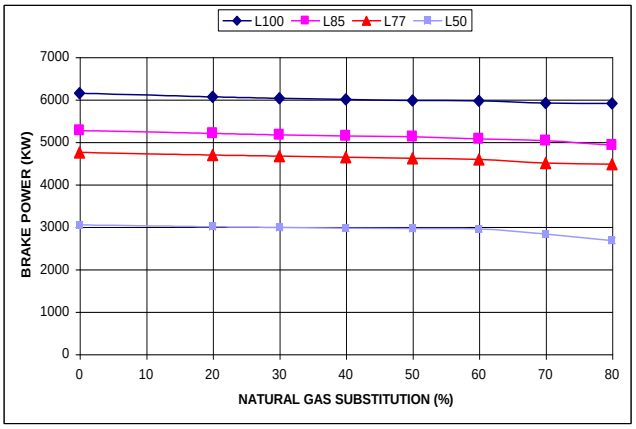

Figure 1: Trends of engine brake power with varying natural gas substitution

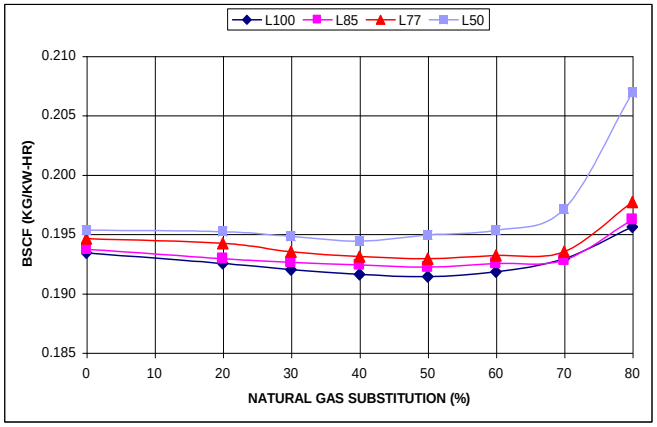

Figure 2: Trends of brake specific fuel consumption with varying natural gas substitution

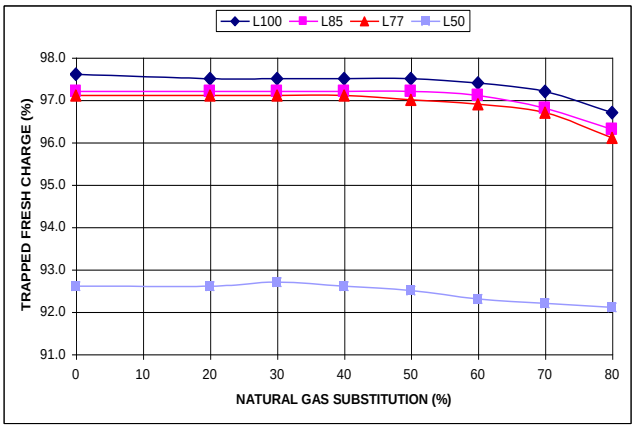

Figure 3: Trends of trapped fresh charge with varying natural gas substitution

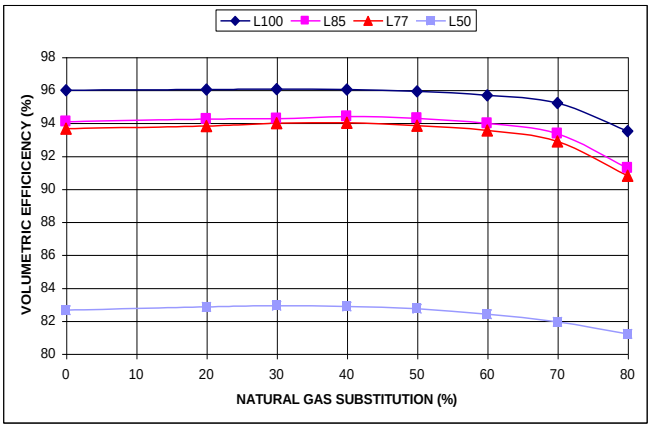

Figure 4: Trends of volumetric efficiency with varying natural gas substitution

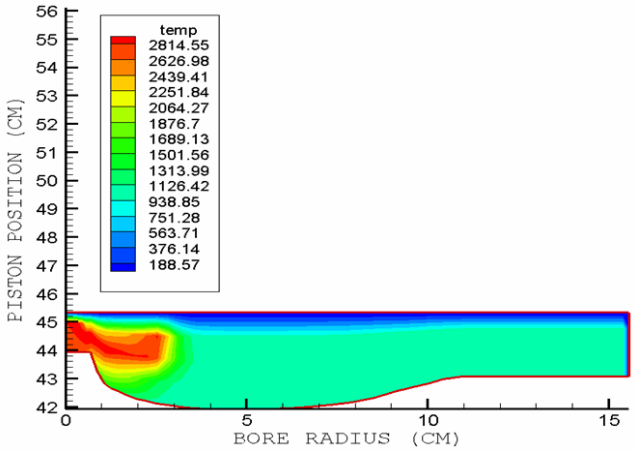

Figure 5: Temperature distribution (Load 85%, Diesel 100%, NG 0%)

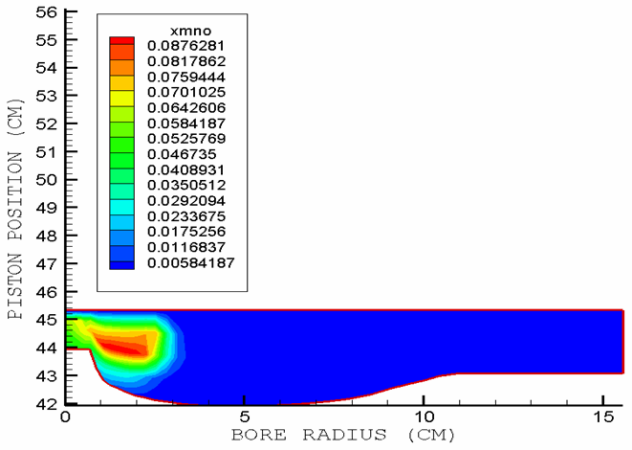

Figure 7: NOx distribution (Load 85%, Diesel, NG 0%)

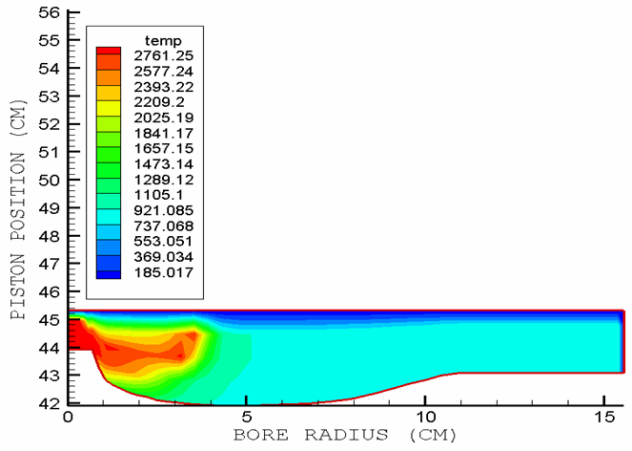

Figure 6: Temperature distribution (Load 85%, Diesel 40%, NG 60%

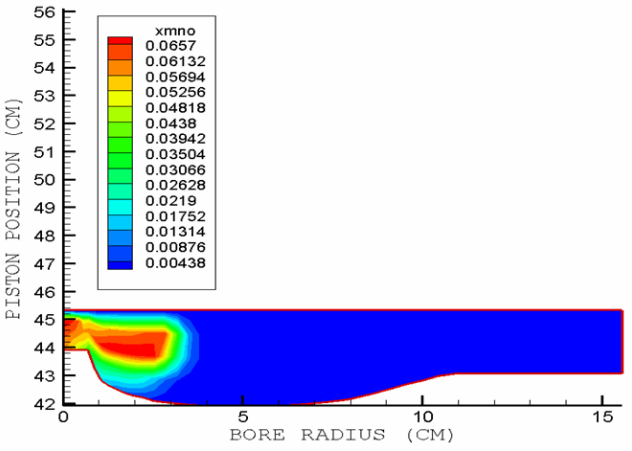

Figure 8: NOx distribution (Load 85%, Diesel 40%, NG 40%)

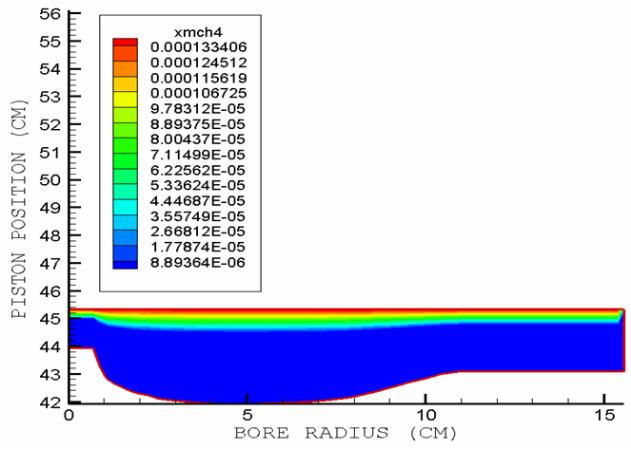

Figure 9: Distribution of unburned natural gas (Load 85%, Diesel 40%, NG 60%)

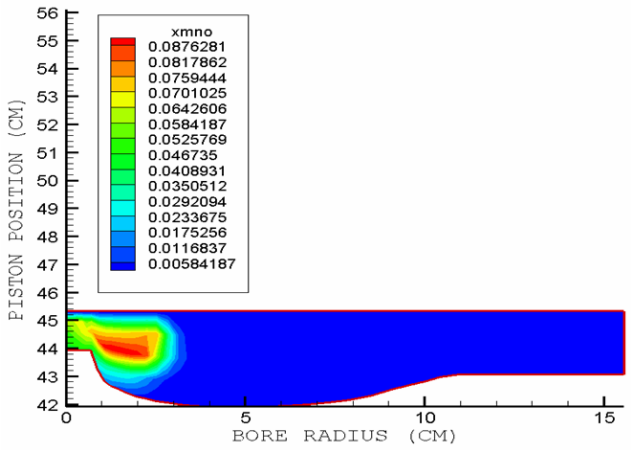

Figure 10: Distribution of unburned natural gas (Load 85%, Diesel 20%, NG 80%)

REFERENCES

[1]. Amsden A. A. and O'Rouke P. J., et al (1989). KIVA-II: A Computer Program for Chemically Reactive Flows with Sprays. LA-11560-MS, May 1989, Los Alamos National Laboratory

[2]. Brombacher, E.J. (1997). Flow Visualisation of Natural Gas Fuel Injection, MSc Thesis, University of Toronto.

[3]. Chiu, J.P. (2004). Low Emissions Class 8 Heavy-Duty, On-Highway Natural Gas and Gasoline Engine. SAE Paper. 2004-01-2982.

[4]. Durell, Elizabeth., Allen, Jeff., Law, Donald., Heath, John: Installation and Development of a Direct Injection System for a Bi-Fuel Gasoline and Compressed Natural Gas Engine, Proceeding ANGVA 2000 Conference, Yokohama, Japan.

[5]. Ganesan, V. Internal Combustion Engines, Second Edition, Tata McGraw-Hill, New Delhi (1999)

[6]. GT-Power: http://www.gtisoft.com/

[7]. Han Z. and Reitz R.D. (1995): Turbulence Modeling of Internal Combustion Engines Using the RNG-$k-\varepsilon$. Combust. Sci. and Tech. **106**: 267-295.

[8]. Han Z. and Reitz R.D. (1997): "A Temperature Wall Function for Variable Density Turbulent Flows with Application to Engine Convective Heat Transfer Modeling". Int. J. H&M Transfer **40**: 613-625

[9]. Heywood, J.B., 1998. Internal Combustion Engine Fundamentals, McGraw-Hill, Singapore

[10]. Kato, K.; Igarashi, K.; Masuda, M.; Otsubo, K.; Yasuda, A.; Takeda, K.; Sato, T. (1999). Development of engine for natural gas vehicle. SAE Paper. 1999-01-0574.1999.

[11]. O'Rouke P. J. and Amsden A. A. (1987). The TAB Method for Numerical Calculation of Spray Droplet Breakup, SAE Paper 87089.

[12]. O'Rourke, P. J. & Bracco, F. V. (1980). Modeling of drop interactions in thick sprays and comparison with experiment. Stratified Charge Automotive Engines Conf., IMechE, Paper No. C404/80.

[13]. Oullette, P.; Mtui, P.L.; Hill, P.G. (1998). Numerical Simulation of Directly Injected Natural Gas and Pilot Diesel Fuel in a Two Stroke Compression Ignition Engine. State of Alternative Fuel Technologies. SAE Paper 981400.

[14]. Pischinger, S., Umierski, M., Hüchtebrock, B (2003). New CNG concepts for passenger cars: High torque engines with superior fuel consumption. SAE Paper 2003-01- 2264.

[15]. Poulton, M.L. (1994). Alternative Fuels for Road Vehicles, Computational Mechanics Publication, London.

[16]. Reitz, R.D. and Diwakar, R., "Structure of High Pressure Fuel Sprays," SAE Paper 870598, (1998).

[17]. Shenghua L, Longbao Z, Ziyan W and R. Jian Combustion Characteristics of Compressed Natural Gas/Dieasel Turbocharged Compressed Ignition Engine, proc Inst Engrs Part D: J Autom Eng, 217 (2003) 833-838

[18]. W. E. Ranz and W. R. Marshall, Jr. Evaporation from Drops, Part I. Chem. Eng. Prog., 48(3):141-146, March 1952.